ACS APPLIED MATERIALS & INTERFACES
Research Article
www.acsami.org

In Situ Catalytic Synthesis of High-Graphitized Carbon-Coated $LiFePO_4$ Nanoplates for Superior Li-Ion Battery Cathodes

Zhipeng Ma,[†,‡] Yuqian Fan,[†,‡] Guangjie Shao,*[,†,‡] Guiling Wang,[†,‡] Jianjun Song,[†,‡] and Tingting Liu[†,‡]

[†]State Key Laboratory of Metastable Materials Science and Technology, Yanshan University, Qinhuangdao 066004, China
[‡]Hebei Key Laboratory of Applied Chemistry, College of Environmental and Chemical Engineering, Yanshan University, Qinhuangdao 066004, China

Supporting Information

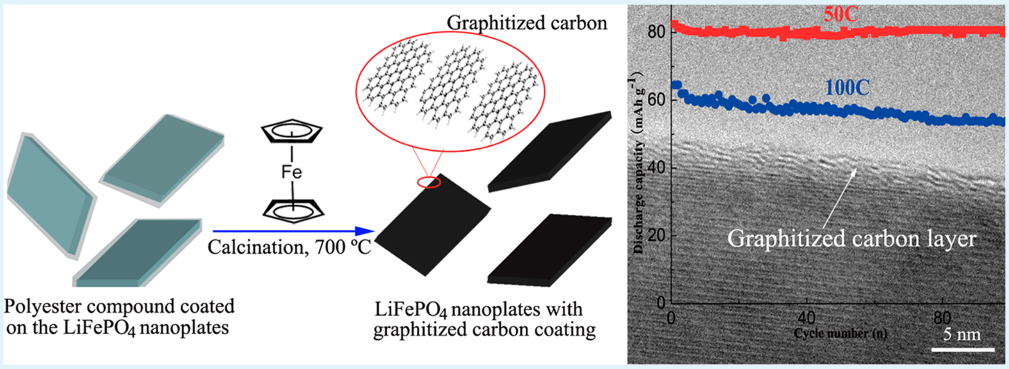

ABSTRACT: The low electronic conductivity and one-dimensional diffusion channel along the *b* axis for Li ions are two major obstacles to achieving high power density of $LiFePO_4$ material. Coating carbon with excellent conductivity on the tailored $LiFePO_4$ nanoparticles therefore plays an important role for efficient charge and mass transport within this material. We report here the in situ catalytic synthesis of high-graphitized carbon-coated $LiFePO_4$ nanoplates with highly oriented (010) facets by introducing ferrocene as a catalyst during thermal treatment. The as-obtained material exhibits superior performances for Li-ion batteries at high rate (100 C) and low temperature (−20 °C), mainly because of fast electron transport through the graphitic carbon layer and efficient Li^+-ion diffusion through the thin nanoplates.

KEYWORDS: *lithium−iron phosphate, carbon coating, graphitization, high rate, low temperature*

1. INTRODUCTION

Nowadays, although Li-ion battery technology is sufficient to power small portable devices such as mobile phones and laptop computers, significant challenges in the specific capacity and rate capability (the energy and power density) must be overcome to expand applications in electric and hybrid electric vehicles. Olivine-structured $LiFePO_4$ is one of the most promising cathode materials for next-generation Li-ion batteries in applications of large-size and high-power devices.[1] Compared with commercial-layered $LiCoO_2$ material with lower capacity and poorer safety, it possesses more excellent chemical and thermal stability, an acceptable flat voltage plateau (3.4 V vs Li^+/Li), and a high theoretical rate capacity of 170 mAh g^{-1}, and it offers economic and environmental advantages because of its low cost and nontoxicity. However, the undesirable high-rate and low-temperature performances of $LiFePO_4$ resulting from its poor electronic conductivity nature and sluggish ionic diffusion along the *b* axis restrict its applications in large power devices.[2] The key issues are how fast Li^+ ion inserted/extracted and how fast electrons can be transported during the charge/discharge process.

Enormous efforts have been made to improve the electronic and ionic conductivity of the bulk as well as surface of the $LiFePO_4$ material using different modification methods.[3−20] Coating carbon and controlling the orientation of the $LiFePO_4$ crystals are two major methods to obtain good electrochemical performance. In the past decades, olivine $LiFePO_4$ with a variety of particle morphologies and sizes has been easily synthesized by hydrothermal techniques; for instance, $LiFePO_4$ crystallites with plate,[10−12] nanorod,[13−15] mesoporous microsphere,[16,17] folwer-like,[18,19] and cagelike[20] structures. Besides, computational[21,22] and experimental[23] studies of $LiFePO_4$ have indicated that charge transfer mainly takes place on the *ac* facet, and Li^+ ion migration occurs preferentially via one-dimensional channels oriented along the [010] direction of the orthorhombic crystal structure during charge and discharge. Thus, nanoparticles with a short *b* axis are ideal structures for a good electrochemical performance of $LiFePO_4$.

Received: December 1, 2014
Accepted: January 13, 2015
Published: January 13, 2015

DOI: 10.1021/am5084368
ACS Appl. Mater. Interfaces 2015, 7, 2937−2943

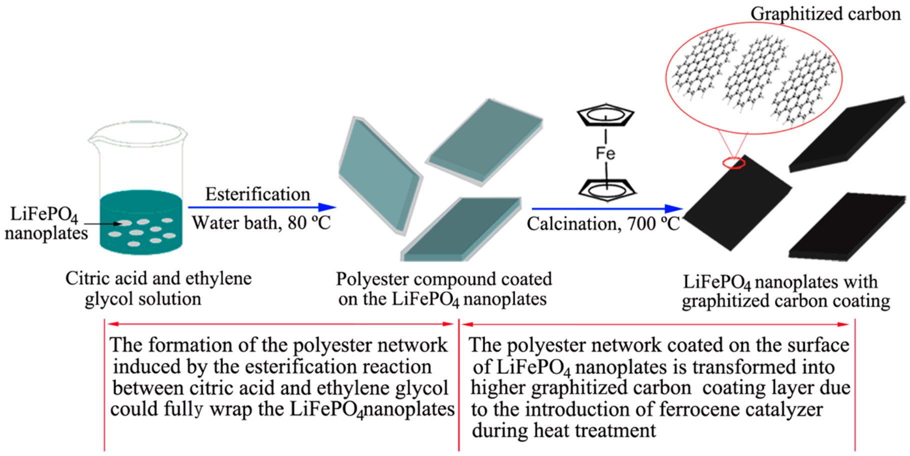

Figure 1. Schematic illustration of the preparation process for the $LiFePO_4$ nanoplates with a graphitized carbon coating.

Although considerable progress has been made in the tunable morphology synthesis of $LiFePO_4$ nanoparticles, the tailored $LiFePO_4$ nanoparticles uniformly and entirely coated with high conductivity carbon remain unanswered. In particular, the effectiveness of the carbon layer in enhancing the electrochemical performances of $LiFePO_4$ can be affected by many factors, such as the content,[24] thickness,[25] morphology,[9,26] and distribution[27] of carbon, especially carbon characteristics (graphitic carbon is more desirable because of its excellent electronic conductivity).[28,29] In comparison with the amorphous carbon, it was demonstrated that the graphitic carbon could lead to more apparent improvement in the electrochemical properties of $LiFePO_4$. For example, some researchers used $LiFePO_4$/reduced graphene oxide (rGO) hybrids as cathode materials for Li-ion batteries with outstanding rate performances, in which the cathode was prepared either by the mechanical mixing of rGO with $LiFePO_4$ particles[30] or by pyrolysis of GO/rGO with either $LiFePO_4$ precursor or $LiFePO_4$ particles.[29,31−39] In addition, the different structure of $LiFePO_4$/carbon nanotube (CNT) hybrid composites (for instance, $LiFePO_4$ microsphere cathode materials with CNT networks embedded,[40] a coaxial-type CNT embedding $LiFePO_4$ nanocomposites,[41] a porous $LiFePO_4$/CNT composite,[42] and core−shell $LiFePO_4$@CNT nanowires[28]) have also been reported for an improved electrochemical performance. It is noted that most of the above-mentioned $LiFePO_4$ was directly modified by graphitic carbon, which was preprepared. Moreover, the surface of $LiFePO_4$ was not fully coated by graphitic carbon. However, the method in which the high-graphitized carbon coating layer on the $LiFePO_4$ surface was in situ synthesized has been scarcely reported.

In this paper, we report on the in situ catalytic synthesis of high-graphitized carbon-coated $LiFePO_4$ nanoplates with highly oriented (010) facets, and their application as a cathode material for superior high-performance Li^{+} ion batteries. Ferrocene was adopted as the catalyst in order to obtain a high-graphitized carbon layer on $LiFePO_4$ nanoplates. The several nanometers thick carbon layer (the equivalent of rGO prepared by the chemical method) with high electronic conductivity could then greatly facilitate the kinetics by ensuring sufficient electron supply and fast Li-ion penetration for the $LiFePO_4$ electrode, especially at super high rate (100 C) and low temperature (−20 °C).

2. EXPERIMENTAL SECTION

2.1. Material Preparation and Characterization. $LiFePO_4$ nanoplates were prepared by the solvothermal route with ethylene glycol (EG) as the reaction medium solvent. For a typical synthesis, 0.0405 mol of $LiOH{\cdot}H_2O$ was dissolved in 20 mL of EG. Then 0.0225 mol of H_3PO_4 was added to the LiOH solution under stirring to form a white deposit. Afterward, 0.015 mol of $FeSO_4{\cdot}7H_2O$ dissolved in 20 mL of EG was dropped into the above suspension with vigorous magnetic stirring for 30 min. The precursor was transferred into a Teflon-lined autoclave (inner volume: 100 mL), heated to 180 °C for 18 h, and then cooled to room temperature. The obtained precipitate was filtered and washed several times with distilled water and ethanol and dried at 80 °C for 12 h.

In order to achieve high-graphitized carbon-coated $LiFePO_4$ nanoplates, $LiFePO_4$ nanoplates (0.4 g) and the proper amount of EG (0.21 g) were added to 10 mL of a citric acid (0.18 g) solution under stirring, and then the solution was evaporated at 80 °C in a water bath to obtain the $LiFePO_4$ nanoplates wrapped with a polyester compound of a dark-blue-gel state. After that, the $LiFePO_4$ nanoplates wrapped with polyester compound were added with 1 wt % ferrocene, and then the mixture was carbonized for 6 h at 700 °C in a stainless steel reactor under a nitrogen atmosphere to obtain high-graphitized carbon-coated $LiFePO_4$ nanoplates (denoted as $LiFePO_4$/FC), as shown in Figure 1. For the sake of comparison, the $LiFePO_4$/C products were synthesized by directly heating the polyester-compound-coated $LiFePO_4$ nanoplates.

The X-ray diffraction (XRD) patterns were characterized on a Rigaku Smart Lab X-ray diffractometer operated at 40 kV using Cu Kα radiation at a scan rate of 5° min^{-1}. Raman spectra were obtained by using a Renishaw Invia Raman microscope instrument equipped with an Ar^{+} laser (λ = 514.5 nm) at 10% and 100% power in the range of 100−3500 cm^{-1}. The morphology and microstructure of the powders were observed by field-emission scanning electron microscopy (FE-SEM) on a S-4800 microscope and high-resolution transmission electron microscopy (HRTEM) with a model JEM2010 microscope.

2.2. Cell Fabrication and Electrochemical Analysis. The electrochemical performances of the samples were measured in a simulative cell consisting of a working electrode and a Li foil electrode separated by a Celgard 2400 microporous membrane. The working electrode was prepared by dispersing 80 wt % active materials, 10 wt % acetylene black, and 10 wt % poly(vinylidene fluoride) binder in the *N*-methylpyrrolidione solvent to form a uniform slurry. The slurry was coated on Al foils and dried in a vacuum at 120 °C for 12 h. The electrolyte was 1 M $LiPF_6$/EC + DEC (1:1, v/v). The cells were assembled in an argon-filled glovebox and tested by galvanostatic charge/discharge cycling in the voltage ranges of 2.4−4.2 and 2.2−4.5 V on a battery testing system (LAND, Wuhan, China). In the test, the mass loading of active material was controlled at 2 mg on a cathode with a surface area of 0.785 cm^2. The electrochemical impedance spectroscopy (EIS) test (the frequency range of 0.01−100000 Hz) was performed on a ParStat 4000 electrochemical workstation.

3. RESULTS AND DISCUSSION

The phase purity and crystal structure of the products were examined by XRD. Figure 2a shows that the XRD patterns of pure $LiFePO_4$, $LiFePO_4/C$, and $LiFePO_4/FC$ products can be indexed as an orthorhombic *Pnma* space group (JCPDS card no. 83-2092). To investigate the surface distribution and degree of graphitization of the carbon layer, Raman spectra of the $LiFePO_4$ products before and after carbon coating were measured, as shown in Figure 2b. It is found that a strong Raman peak around 949 cm^{-1} and a number of weak peaks at 628, 995, and 1067 cm^{-1} are detected for the pure $LiFePO_4$ nanoplates. For the $LiFePO_4$ nanoplates after carbon coating, the area ratio of the D band to the G band (A_D/A_G = 2.1 obtained by fitting D and G bands using Gaussian profile) in $LiFePO_4/FC$ is lower than that obtained in $LiFePO_4/C$ (A_D/A_G = 2.9), which suggests that more graphitized carbon can be obtained by the catalytic action of ferrocene. Moreover, no Raman signals of $LiFePO_4$ can be distinguished in the Raman spectra of $LiFePO_4/C$ or $LiFePO_4/FC$. This result well illuminates that the carbon layers are fully coated on the surface of $LiFePO_4$, which shields the inner $LiFePO_4$ from being detected. In addition, the spectra of the $LiFePO_4$ nanoplates after carbon coating under a high-energy laser, presented in Figure S1 (Supporting Information), displays some peaks of anamorphic PO_4^{3-} as well as Fe^{2+}. This is deduced to result from some oxidization reaction on the surface of $LiFePO_4$ during the process of high-energy lasering. Interestingly, the D and G bands for $LiFePO_4/FC$ remain, while the D and G bands of $LiFePO_4/C$ disappear. This also indicates that the degree of graphitization of the carbon-coating layer on $LiFePO_4/FC$ is higher than that of the carbon-coating layer on $LiFePO_4/C$. The (002) peak of graphite is found in the XRD profile of FC in Figure S2 (Supporting Information). It further suggests that the introduction of the ferrocene catalyst during heat treatment can improve the degree of graphitization of the carbon.

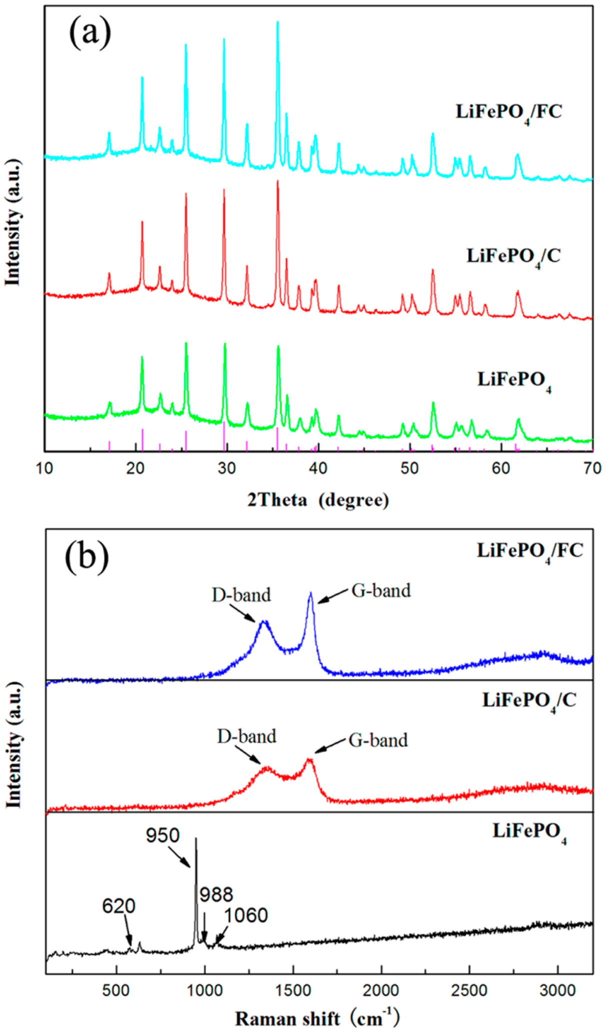

Figure 2. XRD profiles (a) and Raman spectra (b) of pure $LiFePO_4$, $LiFePO_4/C$, and $LiFePO_4/FC$ products.

The particle size, morphology, and crystal orientation of the $LiFePO_4$ and $LiFePO_4/FC$ nanoplates are provided by SEM and TEM, as shown in Figure 3. It can be seen from Figure 3a that the as-prepared $LiFePO_4$ particles present a particular plate morphology with a thickness of 25 nm. However, further investigation on the crystal orientation of $LiFePO_4$ nanoplates demonstrates that the most of the exposing facets are the (010) crystal face, which is favorable for fast Li^+-ion diffusion along the [010] direction during the charge/discharge process. After calcination and carbon coating, both of the $LiFePO_4/FC$ (Figure 3b) and $LiFePO_4/C$ (Figure S3 in the Supporting Information) products retain platelike morphology and show quite similar thickness (around 34 nm). In addition, it can be seen from HRTEM (Figure 3d) that the graphitized carbon coating layer with a thickness of 2 nm was coated on the surface of the $LiFePO_4$ nanoplates uniformly. According to the fast Fourier transform pattern in the inset of Figure 3d, the lattice spacing of 0.47 nm could be assigned to the (001) crystal plane. Moreover, the amount of coated carbon on the $LiFePO_4$ nanoplates is checked by thermogravimetric analysis (TGA; see Figure S4 in the Supporting Information for more details). The percentages of coated carbon in the $LiFePO_4/FC$ and $LiFePO_4/C$ nanoplates are ca. 5.8 and 5.49 wt %, respectively.

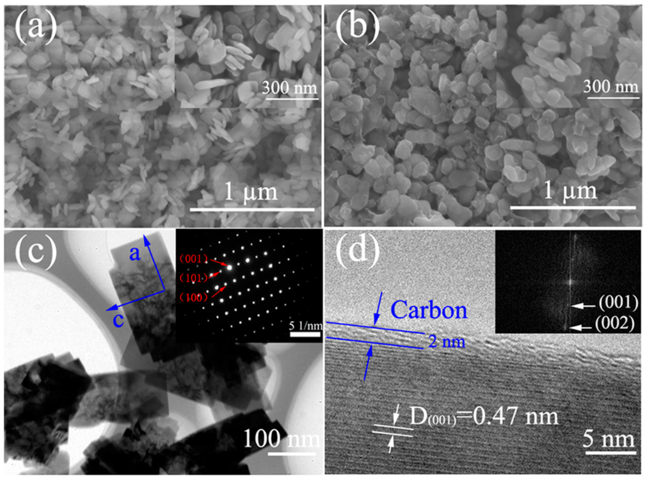

Figure 3. Typical SEM images of (a) $LiFePO_4$ and (b) $LiFePO_4/FC$ nanoplates. (c) TEM image of $LiFePO_4$ nanoplates (the inset image is the corresponding selected-area electron diffraction pattern). (d) HRTEM image of $LiFePO_4/FC$ nanoplates (the inset image is the corresponding fast Fourier transform pattern).

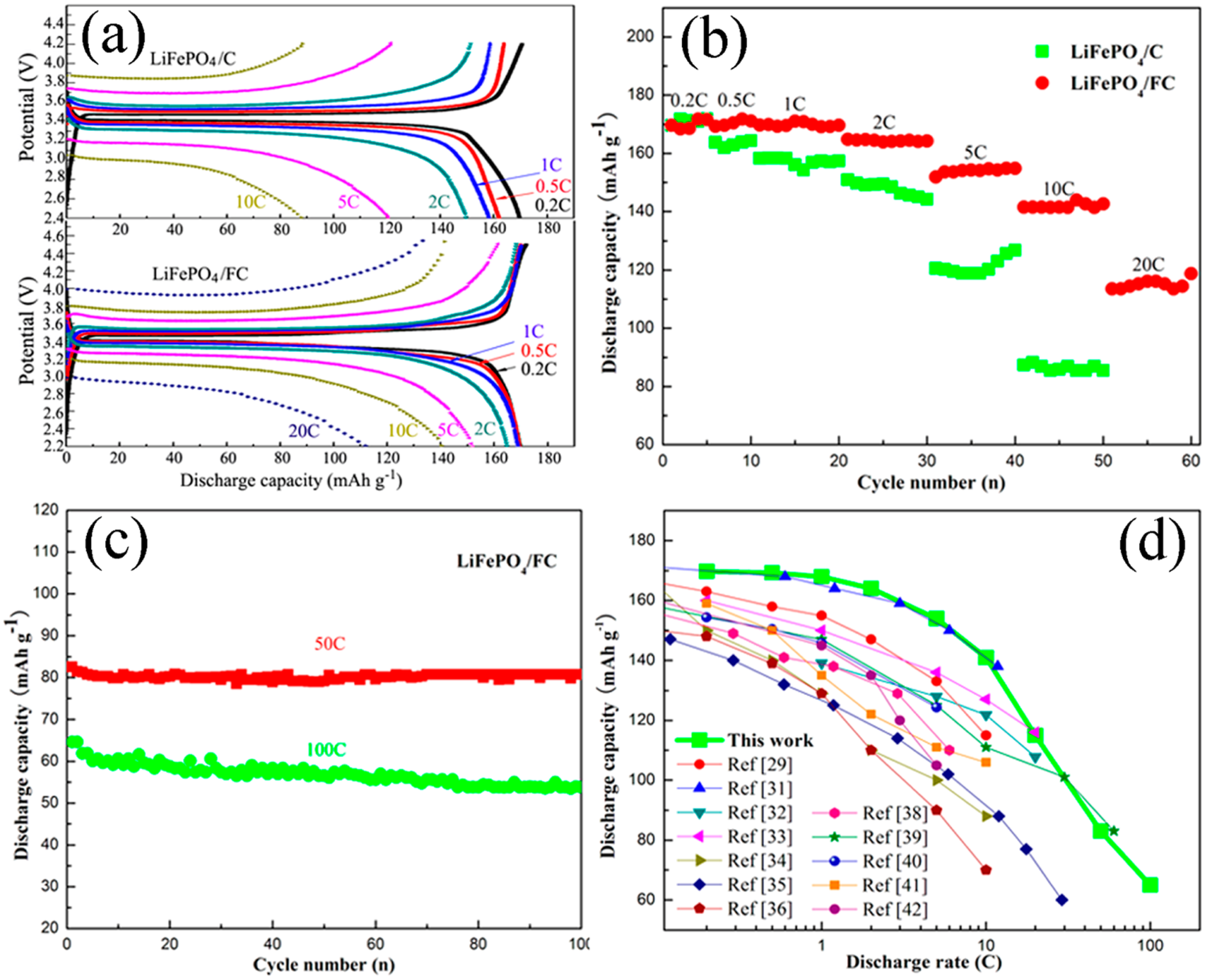

Figure 4. (a) Typical charge/discharge curves and (b) rate performances of the $LiFePO_4$/C and $LiFePO_4$/FC nanoplate electrodes, (c) specific capacity retention of the $LiFePO_4$/FC nanoplate electrode at superior high rate, and (d) high rate capability of the $LiFePO_4$/FC nanoplate electrode and those reported previously.

To demonstrate the hypothesis that a superior electrochemical performance of $LiFePO_4$/FC nanoplates could be achieved by a higher graphitized carbon layer coating on their surface, $LiFePO_4$/C nanoplates without the introduction of a ferrocene catalyst during the coating carbon process were prepared as references. Parts a and b of Figure 4 show the initial charge/discharge curves and cycle capability of the $LiFePO_4$/FC and $LiFePO_4$/C nanoplate electrode at various rates, respectively. At low or moderate current densities, both electrodes show comparable reversible capacities, for instance, 169.7 and 168 mAh g^{-1} for $LiFePO_4$/FC nanoplates and 169.6 and 160 mAh g^{-1} for $LiFePO_4$/C nanoplates at discharge rates of 0.2 and 1 C, respectively. When the discharge rate is higher than 2 C, t the difference in the rate performance between the two electrodes becomes obvious. The $LiFePO_4$/FC nanoplate electrode presents a high discharge capacity of ca. 164, 154, 141, and 114 mAh g^{-1} at 2, 5, 10, and 20 C rate, respectively, while the $LiFePO_4$/C nanoplate electrode only exhibits ca. 148, 119, and 85 mAh g^{-1} at rates of 2, 5, and 10 C, respectively. Noticeably, a more stable potential plateau during the charge/discharge process for the $LiFePO_4$/FC nanoplate electrode indicates a more alleviated polarization due to the high graphitic carbon layer. Moreover, it is noticeable that the cycle capability of the $LiFePO_4$/FC nanoplate electrode at high rate is superior to that of $LiFePO_4$/C (Figure 4b). To further test the potential applicability of the $LiFePO_4$/FC nanoplate electrode at a super high rate, the average reversible capacity of the $LiFePO_4$/FC nanoplate electrode achieves 82.5 and 64.5 mAh g^{-1} at the super high rates of 50 and 100 C, respectively, as shown in Figure 4c. The corresponding Coulombic efficiency after 100 cycles is ca. 98% and 88%, respectively. Figure 4d compares the high rate capability of the $LiFePO_4$/FC nanoplates with those previously reported on $LiFePO_4$ and graphitic carbon hybrid composites. Among those composites, the electrodes prepared with $LiFePO_4$ directly modified by CNT and rGO exhibited fairly good rate performance.[30,31,40−42] Particularly, the $LiFePO_4$ nanoplates ($LiFePO_4$/FC nanoplates) fully coated with the in situ catalytic synthesized high-graphitized carbon exhibited a far better high rate capability over the range of discharge rate up to 100 C. This superior rate performance is attributed to the excellent electronic conductivity of the high-graphitized thin carbon layer, which favors ion transportation. Moreover, the carbon contents also influence the electrochemical performance of $LiFePO_4$. The carbon contents of $LiFePO_4$/graphitic carbon hybrid composites in the previous reports are shown in Table 1. It can be seen from Table 1 that the good electrochemical performance of the $LiFePO_4$/CNT and $LiFePO_4$/graphene composites in the previous reports is attributed to the high carbon content. However, it is deduced that the tap density of

Table 1. Discharge Capacity and Carbon Content for Different Samples

sample	synthetic method	capacity, mAh g^{-1} (rate, C)	carbon content, wt %	tap density, g cm^{-3}
$LiFePO_4$/FC (this work)	solvothermal method	141 (10)	5.8	1.2
$LiFePO_4$/CNT[37]	precipitation method	139 (10)	23.8	no report
$LiFePO_4$/rGO[31]	precipitation method	139 (11.8)	15	no report
$LiFePO_4$/graphene[35]	hydrothermal method	ca. 90 (11.8)	19.8	no report
$LiFePO_4$/C/graphene[34]	hydrothermal method	88 (10)	5	no report
$LiFePO_4$/CNT[36]	hydrothermal method	88 (5)	6.84	no report

the $LiFePO_4$/CNT and $LiFePO_4$/graphene composites is low due to the high carbon content, whereas when the carbon content is low, the electrochemical performance of the $LiFePO_4$/CNT and $LiFePO_4$/graphene composites is far worse than that of the $LiFePO_4$/FC nanoplates in our study. For the $LiFePO_4$/FC nanoplates, the low carbon content (only 5.8 wt %) and the high tap density (1.2 g cm^{-3}) are two key factors for the practical application of Li-ion battery with high energy density.

In addition, a low-temperature performance is also important for application of the $LiFePO_4$ cathode material in Li^+-ion batteries. Figure 5 shows the rate capability and typical charge/discharge profiles of the $LiFePO_4$/FC and $LiFePO_4$/C nanoplate electrodes at −20 °C. It is obvious that the $LiFePO_4$/FC nanoplate electrode exhibits discharge capacities of 139.3, 123.6, 109.2, and 92.47 mAh g^{-1} at 0.2, 0.5, 1, and 2 C, respectively, which are much higher than those of the $LiFePO_4$/C nanoplate electrode, which displays capacities of 133, 111, 86.3, and 61.5 mAh g^{-1}. The $LiFePO_4$/FC nanoplate electrode even shows capacities of 72 and 44 mAh g^{-1} at 5 and 10 C, respectively, but the $LiFePO_4$/C nanoplate electrode can hardly recharge at 5 C. Apparently, the low-temperature performance of the $LiFePO_4$ nanoplates is improved by the coating of a graphitic carbon layer.

To further understand the superior electrode performance of the $LiFePO_4$/FC nanoplates, we carried out electrochemical cyclic voltammetry and EIS, as illustrated in Figure 6a,b. Cyclic voltammetry profiles at a low scan rate of 0.5 mV s^{-1} indicated that the potential interval between the cathodic and anodic peaks for $LiFePO_4$/FC and $LiFePO_4$/C nanoplate electrodes are comparable. However, the redox peak curve of the $LiFePO_4$/FC nanoplate electrode is sharper and more symmetric than that of the $LiFePO_4$/C nanoplate electrode, suggesting that the redox kinetics of the $LiFePO_4$/FC nanoplate electrode is enhanced because of the improvement of graphitization of the carbon layer. Moreover, the $LiFePO_4$/FC nanoplate electrode delivers a lower charge-transfer resistance compared with that of the $LiFePO_4$/C nanoplate electrode in Figure 6b. The fitting value of the charge-transfer resistance for the $LiFePO_4$/FC nanoplate electrode is 139.5 Ω,

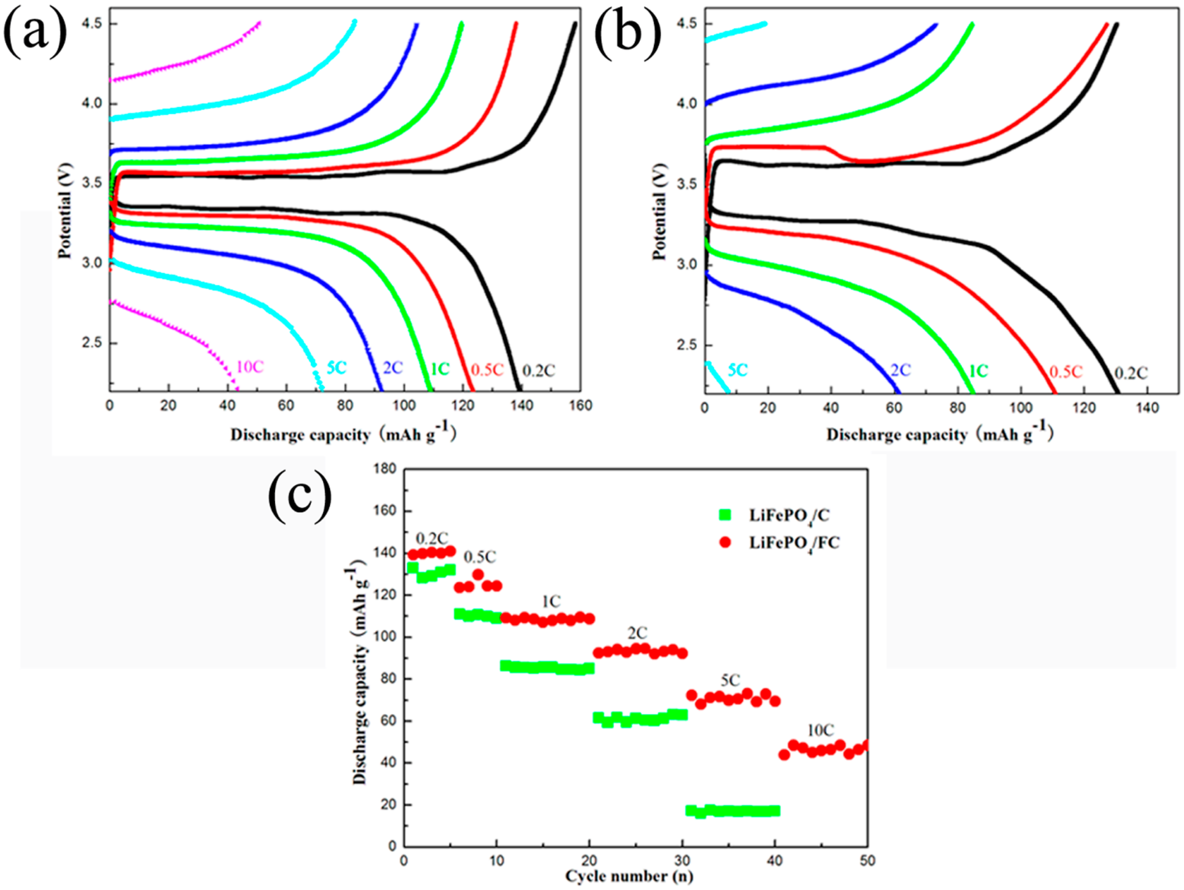

Figure 5. Typical charge/discharge profiles of the $LiFePO_4$/FC (a) and $LiFePO_4$/C (b) nanoplate electrodes at −20 °C and the rate capability of the $LiFePO_4$/FC and $LiFePO_4$/C nanoplate electrodes at −20 °C (c).

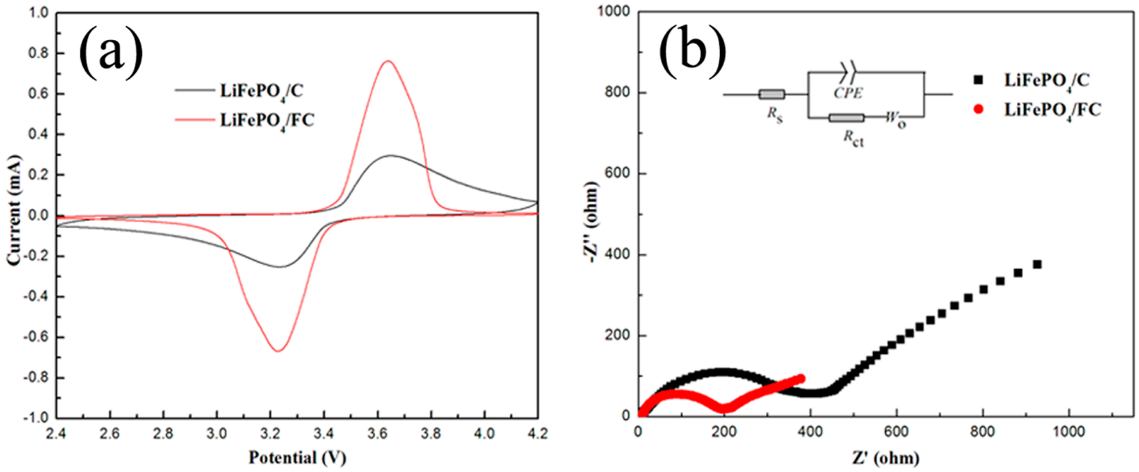

Figure 6. Cyclic voltammetry (a) and EIS measurements (b) of the $LiFePO_4/C$ and $LiFePO_4/FC$ nanoplate electrodes.

superior to 367.9 Ω of the $LiFePO_4/C$ nanoplate electrode. According to the slopes of the part of the electrochemical impedance versus the square root of the frequency (see Figure S5 in the Supporting Information for more details), the Li-ion diffusion coefficients of the $LiFePO_4/FC$ and $LiFePO_4/C$ nanoplate electrodes were calculated to be 4.27×10^{-14} and 3.61×10^{-15} cm^2 s^{-1}, respectively. These results indicate that the coating of high-graphitized carbon onto the surface of the $LiFePO_4$ nanoplates can improve diffusion of the Li^+ ion during the charge/discharge process.

4. CONCLUSIONS

In summary, high-graphitized carbon-coated $LiFePO_4$ nanoplates were synthesized via the introduction of a ferrocene catalyst during heat treatment. This material exhibits an outstanding electrochemical performance with a high specific capacity that is comparable to the theoretical capacity at low or moderate rate, a superior high rate capability, a remarkable low-temperature property, and good capacity retention. The excellent properties can be attributed to the graphitized carbon layer coating on the surface of the $LiFePO_4$ nanoplates, which can transport the electron and Li^+ ion at a high speed during the charge/discharge process.

■ ASSOCIATED CONTENT

Ⓢ Supporting Information

Additional XRD, Raman spectra, SEM, TEM, TGA, and EIS data. This material is available free of charge via the Internet at http://pubs.acs.org.

■ AUTHOR INFORMATION

Corresponding Author

*E-mail: shaoguangjie@ysu.edu.cn. Tel.: 0086-335-8061569. Fax: 0086-335-8059878.

Notes

The authors declare no competing financial interest.

■ ACKNOWLEDGMENTS

We are grateful for financial support from the Natural Science Foundation of Hebei Province (Grants B2012203069 and B2012203070) and support from the education department of Hebei Province on natural science research key projects for institution of higher learning (Grant ZH2011228).

■ REFERENCES

(1) Padhi, A. K.; Nanjundaswamy, K. S.; Goodenough, J. B. Phospho-Olivines as Positive-Electrode Materials for Rechargeable Lithium Batteries. *J. Electrochem. Soc.* **1997**, *144*, 1188−1194.

(2) Yuan, L. X.; Wang, Z. H.; Zhang, W. X.; Hu, X. L.; Chen, J. T.; Huang, Y. H.; Goodenough, J. B. Development and Challenges of $LiFePO_4$ Cathode Material for Lithium-ion Batteries. *Energy Environ. Sci.* **2011**, *4*, 269−284.

(3) Wu, Y.; Wen, Z.; Li, J. Hierarchical Carbon-coated $LiFePO_4$ Nanoplate Microspheres with High Electrochemical Performance for Li-ion Batteries. *Adv. Mater.* **2011**, *23*, 1126−1129.

(4) Sun, C.; Rajasekhara, S.; Goodenough, J. B.; Zhou, F. Monodisperse Porous $LiFePO_4$ Microspheres for a High Power Li-ion Battery Cathode. *J. Am. Chem. Soc.* **2011**, *133*, 2132−2135.

(5) Bilecka, I.; Hintennach, A.; Rossell, M. D.; Xie, D.; Novak, P.; Niederberger, M. Microwave-assisted Solution Synthesis of Doped $LiFePO_4$ with High Specific Charge and Outstanding Cycling Performance. *J. Mater. Chem.* **2011**, *21*, 5881−5890.

(6) Jiang, Y.; Liao, S.; Liu, Z.; Xiao, G.; Liu, Q.; Song, H. High Performance $LiFePO_4$ Microsphere Composed of Nanofibers with an Alcohol-thermal Approach. *J. Mater. Chem. A* **2013**, *1*, 4546−4551.

(7) Zhao, Y.; Peng, L.; Liu, B.; Yu, G. Single-crystalline $LiFePO_4$ Nanosheets for High-rate Li-ion Batteries. *Nano Lett.* **2014**, *14*, 2849−2853.

(8) Wang, Y. G.; He, P.; Zhou, H. S. Olivine $LiFePO_4$: Development and Future. *Energy Environ. Sci.* **2011**, *4*, 805−817.

(9) Wang, G.; Liu, H.; Liu, J.; Qiao, S.; Lu, G. M.; Munroe, P.; Ahn, H. Mesoporous $LiFePO_4/C$ Nanocomposite Cathode Materials for High Power Lithium Ion Batteries with Superior Performance. *Adv. Mater.* **2010**, *22*, 4944−4948.

(10) Qin, X.; Wang, J.; Xie, J.; Li, F.; Wen, L.; Wang, X. Hydrothermally Synthesized $LiFePO_4$ Crystals with Enhanced Electrochemical Properties: Simultaneous Suppression of Crystal Growth along [010] and Antisite Defect Formation. *Phys. Chem. Chem. Phys.* **2012**, *14*, 2669−2677.

(11) Yang, S.; Zhou, X.; Zhang, J.; Liu, Z. Morphology-controlled Solvothermal Synthesis of $LiFePO_4$ as a Cathode Material for Lithium-ion Batteries. *J. Mater. Chem.* **2010**, *20*, 8086−8091.

(12) Ma, Z.; Shao, G.; Wang, Xu.; Song, J.; Wang, G.; Liu, T. Solvothermal Synthesis of $LiFePO_4$ Nanoplates with (010) Plane and the Uniform Carbon Coated on Their Surface by Esterification Reaction. *Mater. Chem. Phys.* **2014**, *143*, 969−976.

(13) Li, J.; Qu, Q.; Zhang, L.; Zhang, L.; Zheng, H. A Monodispersed Nano-hexahedral $LiFePO_4$ with Improved Power Capability by Carbon-coatings. *J. Alloys Compd.* **2013**, *579*, 377−383.

(14) Liang, Y. P.; Li, C. C.; Chen, W. J.; Lee, J. T. Hydrothermal Synthesis of Lithium Iron Phosphate using Pyrrole as an Efficient Reducing Agent. *Electrochim. Acta* **2013**, *87*, 763−769.

(15) Chen, Q.; Qiao, X.; Peng, C.; Zhang, T.; Wang, Y.; Wang, X. Electrochemical Performance of Electrospun $LiFePO_4/C$ Submicrofibers Composite Cathode Material for Lithium Ion Batteries. *Electrochim. Acta* **2012**, *78*, 40−48.

(16) Cho, M. Y.; Kim, K. B.; Lee, J. W.; Kim, H.; Kim, H.; Kang, K.; Roh, K. C. Defect-free Solvothermally Assisted Synthesis of Microspherical Mesoporous $LiFePO_4/C$. *RSC Adv.* **2013**, *3*, 3421−3427.

(17) Gu, Y.; Liu, W.; Wang, L.; Li, G.; Yang, Y. Synthesis of 3D-hierarchical $LiMPO_4$ (M = Fe, Mn) Microstructures as Cathode Materials for Lithium-ion Batteries. *CrystEngComm* **2013**, *15*, 4865−4870.

(18) Zhou, N.; Uckaker, E.; Wang, H. Y.; Zhang, M.; Liu, S. Q.; Liu, Y. N.; Wu, X.; Cao, G.; Li, H. Additive-free Solvothermal Synthesis of Hierarchical Flower-like $LiFePO_4/C$ Mesocrystal and Its Electrochemical Performance. *RSC Adv.* **2013**, *3*, 19366−19374.

(19) Wang, Q.; Deng, S. X.; Wang, H.; Xie, M.; Liu, J. B.; Yan, H. Hydrothermal Synthesis of Hierarchical $LiFePO_4$ Microspheres for Lithium Ion Battery. *J. Alloys Compd.* **2013**, *553*, 69−74.

(20) Deng, H.; Jin, S.; Zhan, L.; Wang, Y.; Qiao, W.; Ling, L. Synthesis of Cage-like $LiFePO_4/C$ Microspheres for High Performance Lithium Ion Batteries. *J. Power Sources* **2012**, *220*, 342−347.

(21) Islam, M. S.; Driscoll, D. J.; Fisher, C. A. J.; Slater, P. R. Atomic-scale Investigation of Defects, Dopants, and Lithium Transport in the $LiFePO_4$ Olivine-type Battery Material. *Chem. Mater.* **2005**, *20*, 5085−5092.

(22) Morgan, D.; Van der Ven, A.; Ceder, G. Li Conductivity in Li_xMPO_4 (M = Mn, Fe, Co, Ni) Olivine Materials. *Electrochem. Solid-State Lett.* **2004**, *7*, A30−A32.

(23) Nishimura, S.; Kobayashi, G.; Ohoyama, K.; Kanno, R.; Yashima, M.; Yamada, A. Experimental Visualization of Lithium Diffusion in Li_xFePO_4. *Nat. Mater.* **2008**, *9*, 707−711.

(24) Yang, J.; Wang, J.; Tang, Y.; Wang, D.; Li, X.; Hu, Y.; Li, R.; Liang, G.; Sham, T. K.; Sun, X. $LiFePO_4$−graphene as a Superior Cathode Material for Rechargeable Lithium Batteries: Impact of Stacked Graphene and Unfolded Graphene. *Energy Environ. Sci.* **2013**, *6*, 1521−1528.

(25) Huang, Z. D.; Oh, S. W.; He, Y. B.; Zhang, B.; Yang, Y.; Mai, Y. W.; Kim, J. K. Porous C−$LiFePO_4$−C Composite Microspheres with a Hierarchical Conductive Architecture as a High Performance Cathode for Lithium Ion Batteries. *J. Mater. Chem.* **2012**, *22*, 19643−19645.

(26) Zhang, X.; Zhang, X.; He, W.; Yue, Y.; Liu, H.; Ma, J. Biocarbon-coated $LiFePO_4$ Nucleus Nanoparticles Enhancing Electrochemical Performances. *Chem. Commun.* **2012**, *48*, 10093−10095.

(27) Oh, S. W.; Myung, S. T.; Oh, S. M.; Oh, K. H.; Amine, K.; Scrosati, B.; Sun, Y. K. Double Carbon Coating of $LiFePO_4$ as High Rate Electrode for Rechargeable Lithium Batteries. *Adv. Mater.* **2010**, *22*, 4842−4845.

(28) Yang, J.; Wang, J.; Tang, Y.; Wang, D.; Xiao, B.; Li, X.; Li, R.; Liang, G.; Sham, T. K.; Sun, X. In Situ Self-catalyzed Formation of Core−shell $LiFePO_4$@CNT Nanowires for High Rate Performance Lithium-ion Batteries. *J. Mater. Chem. A* **2013**, *1*, 7306−7311.

(29) Zhang, Y.; Chen, L.; Ou, J.; Wang, J.; Zheng, B.; Yuan, H.; Guo, Y.; Xiao, D. Improving the Performance of a $LiFePO_4$ Cathode Based on Electrochemically Cleaved Graphite Oxides with High Hydrophilicity and Good Conductivity. *J. Mater. Chem. A* **2013**, *1*, 7933−7941.

(30) Su, F. Y.; You, C.; He, Y. B.; Lv, W.; Cui, W.; Jin, F.; Li, B.; Yang, Q. H.; Kang, F. Flexible and Planar Graphene Conductive Additives for Lithium-ion Batteries. *J. Mater. Chem.* **2010**, *20*, 9644−9650.

(31) Zhu, X.; Hu, J.; Wu, W.; Zeng, W.; Dai, H.; Du, Y.; Liu, Z.; Li, L.; Ji, H.; Zhu, Y. $LiFePO_4$/reduced Graphene Oxide Hybrid Cathode for Lithium Ion Battery with Outstanding Rate Performance. *J. Mater. Chem. A* **2014**, *2*, 7812−7818.

(32) Liu, T.; Zhao, L.; Zhu, J.; Wang, B.; Guo, C.; Wang, D. The Composite Electrode of $LiFePO_4$ Cathode Materials Modified with Exfoliated Graphene from Expanded Graphite for High Power Li-ion Batteries. *J. Mater. Chem. A* **2014**, *2*, 2822−2829.

(33) Wang, B.; Wang, D.; Wang, Q.; Liu, T.; Guo, C.; Zhao, X. Improvement of the Electrochemical Performance of Carbon-coated $LiFePO_4$ Modified with Reduced Grapheme Oxide. *J. Mater. Chem. A* **2013**, *1*, 135−144.

(34) Shi, Y.; Shi, Y.; Chou, S. L.; Wang, J. Z.; Wexler, D.; Li, H. J.; Wu, Y. Graphene Wrapped $LiFePO_4/C$ Composites as Cathode Materials for Li-ion Batteries with Enhanced Rate Capability. *J. Mater. Chem.* **2012**, *22*, 16465−16470.

(35) Ha, J.; Park, S.-K.; Yu, S.-H.; Jin, A.; Jang, B.; Bong, S.; Kim, I.; Sung, Y.-E.; Piao, Y. A Chemically Activated Graphene-encapsulated $LiFePO_4$ Composite for High-performance Lithium Ion Batteries. *Nanoscale* **2013**, *5*, 8647−8655.

(36) Tan, L.; Tang, Q.; Chen, X.; Hu, A.; Deng, W.; Yang, Y.; Xu, L. Mesoporous $LiFePO_4$ Microspheres Embedded Homogeneously with 3D CNT Conductive Networks for Enhanced Electrochemical Performance. *Electrochim. Acta* **2014**, *137*, 344−351.

(37) Jegal, J. P.; Kim, K. B. Carbon Nanotube-embedding $LiFePO_4$ as a Cathode Material for High Rate Lithium Ion Batteries. *J. Power Sources* **2013**, *243*, 859−864.

(38) Zhou, Y.; Wang, J.; Hu, Y.; Ohayre, R.; Shao, Z. A Porous $LiFePO_4$ and Carbon Nanotube Composite. *Chem. Commun.* **2010**, *46*, 7151−7153.

(39) Mo, R.; Lei, Z.; Rooney, D.; Sun, K. Facile Synthesis of Nanocrystalline $LiFePO_4$/graphene Composite as Cathode Material for High Power Lithium Ion Batteries. *Electrochim. Acta* **2014**, *130*, 594−599.

(40) Liu, H.; Miao, C.; Meng, Y.; Xu, Q.; Zhang, X.; Tang, Z. Effect of Graphene Nanosheets Content on the Morphology and Electrochemical Performance of $LiFePO_4$ Particles in Lithium Ion Batteries. *Electrochim. Acta* **2014**, *135*, 311−318.

(41) Lin, X.; Wu, K.; Shao, L.; Shui, M.; Wang, D.; Long, N.; Ren, Y. In Situ Growth of Coiled Carbon Nanotubes on $LiFePO_4$ as High Performance Lithium Storage Material. *J. Electroanal. Chem.* **2014**, *726*, 71−76.

(42) Manikandan, P.; Periasamy, P.; Jagannathan, R. Sol−gel Synthesis and Impedance Characteristics of Networked Nanocrystalline Olivine Cathode for Li-ion Full Cells. *J. Mater. Chem. A* **2013**, *1*, 15397−15405.